Palaeogeography, Palaeoclimatology, Palaeoecology 440 (2015) 690–695

Contents lists available at ScienceDirect

Palaeogeography, Palaeoclimatology, Palaeoecology

journal homepage: www.elsevier.com/locate/palaeo

A delayed end-Permian extinction in deep-water locations and its relationship to temperature trends (Bianyang, Guizhou Province, South China)

Haishui Jiang [a,b,*], Michael M. Joachimski [c], Paul B. Wignall [d], Muhui Zhang [b], Xulong Lai [a,b]

[a] State Key Laboratory of Biogeology and Environmental Geology, China University of Geosciences, Wuhan 430074, China
[b] School of EarthSciences, China University of Geosciences, Wuhan 430074, China
[c] GeoZentrum Nordbayern, Universität Erlangen-Nürnberg, Schlossgarten 5, 91054 Erlangen, Germany
[d] School of Earth and Environment, University of Leeds, Leeds LS2 9JT, UK

ARTICLE INFO

Article history:
Received 24 July 2015
Received in revised form 30 September 2015
Accepted 1 October 2015
Available online 9 October 2015

Keywords:
Conodont
End-Permian extinction
South China
Bianyang

ABSTRACT

New collecting at a biostratigraphically highly-resolved deep-water section in South China, reveals a brief (a few tens of thousands of years) but measurable delay in extinction timing relative to contemporaneous, shallower water sections. Foraminifers and conodonts in the Bianyang section show a sharp extinction at the top of *Hindeodus changxingensis* Zone, whilst in shallower sections, such as the well-known Meishan GSSP location, these taxa have a major extinction pulse at the top of the preceding *Clarkina yini* Zone. The main end-Permian extinction coincides with the onset of a negative carbon isotope excursion whilst the deep-water extinctions occur around the lowpoint of the carbon isotope curve. Rapidly increasing surface water temperatures, and the effects of deep-water anoxia were all important during the crisis although it is noteworthy that regression and extinction also show a close temporal link.

1. Introduction

The largest mass extinction in geological history, at the Permian–Triassic boundary (PTB), was analysed by Yin et al. (2007), who recognized that a main extinction episode in the latest Permian was followed by an epilogue (recovery) episode and a second extinction in the earliest Triassic. The end-Permian mass extinction coincides with a sharp negative shift in the $\delta^{13}C$ record (e.g., Shen et al., 2013; Shen and Bowring, 2014) at the level of the first appearance of the conodont *Hindeodus changxingensis* Wang (Metcalfe et al., 2007). This is below the first appearance of *Hindeodus parvus* (e.g., Jiang et al., 2007, 2011), which marks the base of the Triassic (Yin et al., 2001). The second extinction occurs at the base of the *Isarcicella isarcica* Zone of the Early Triassic (Song et al., 2013). The nature of diversity trends during the ~200 kyr interval between these crises has not been clearly resolved, although a major rise sea-surface temperature is thought to have occurred (Joachimski et al., 2012). In South China, reported diversity levels remain stable after the first mass extinction as continued species losses are balanced by new appearances (Song et al., 2014). Here, we provide evidence that shows that extinction intensity remained high in this epilogue phase in deep-water locations such as the Bianyang section (Guizhou Province, South China) (Fig. 1). The range of foraminifer and conodont taxa, $\delta^{13}C_{carb}$ and $\delta^{18}O$ of conodont apatite have been studied at this location in order to provide a detailed chronology of extinction, carbon cycle perturbations and ocean temperature evolution during the most severe crisis in Earth history.

2. Geological setting

The Bianyang section was located at the northern margin of the Nanpanjiang Basin, close to the Great Bank of Guizhou (GBG) (Lehrmann et al., 1998; Yan et al., 2013) (Fig. 1). Song et al. (2009) studied the foraminifers from the Late Permian to Early Triassic strata at Bianyang although a high-resolution biostratigraphic framework only became available at this location with the detailed conodont study of Yan et al. (2013) supplemented by our own study reported here. This showed that the basinal Bianyang section has a biostratigraphically complete sedimentary succession.

3. Carbon and oxygen isotope analyses

Carbonate powders were reacted with 100% phosphoric acid at 70 °C using a Gasbench II connected to a ThermoFisher V Plus mass spectrometer. All carbon isotope values are reported in permil relative to V-PDB by assigning $\delta^{13}C$ values of +1.95‰ to NBS19 and −46.6‰ to LSVEC.

* Corresponding author at: State Key Laboratory of Biogeology and Environmental Geology, China University of Geosciences, Wuhan 430074, China.

http://dx.doi.org/10.1016/j.palaeo.2015.10.002
0031-0182/

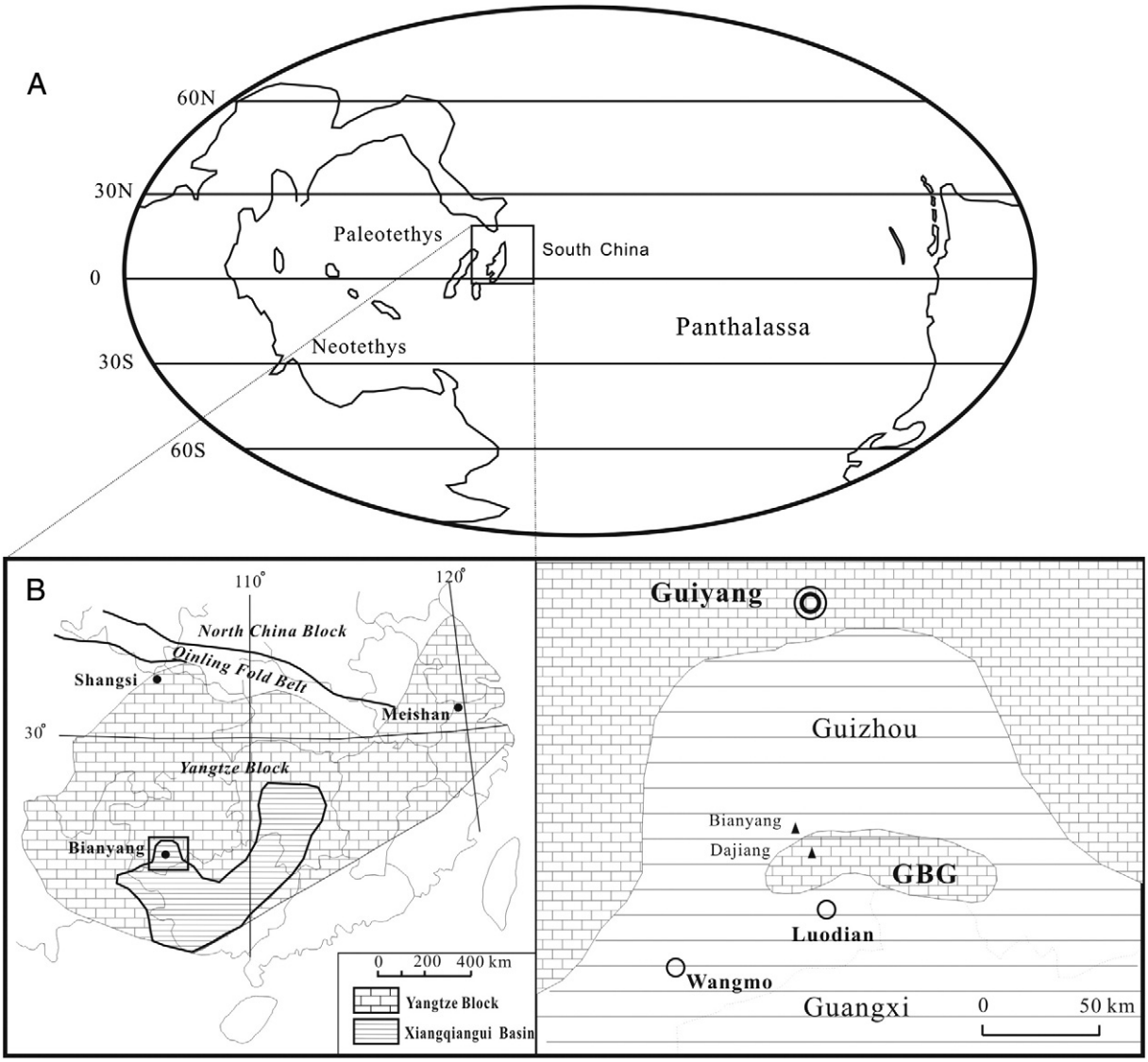

Fig. 1. A, palaeogeography of South China during the Permian–Triassic transitional period (after Stampfli and Borel, 2002; Cavazza et al., 2004); B, modern location of the Bianyang, Dajiang, Meishan and Shangsi sections (modified from Lehrmann et al., 2003; Liu et al., 2007; Jiang et al., 2014). GPS positions, Meishan: N31°04′50.72″, E119°42′21.68″; Shangsi: N32°19′11.28″, E105°27′18.30″; Bianyang: N25°38′41.68″, E106°37′16.28″; Dajiang: N25°33′17.15″, E106°39′43.43″.

Reproducibility and accuracy of carbon isotope analyses were monitored by replicate analysis of laboratory standards calibrated to NBS19 and LSVEC and were ±0.06‰ (1σ).

Oxygen isotope analyses of conodont apatite were performed following the method of Joachimski et al. (2009). Apatite-bound phosphate was converted into trisilverphosphate (Ag_3PO_4) and analysed using a TC-EA (high temperature reduction furnace) coupled online to a ThermoFinnigan Delta Five Plus mass spectrometer. All values are reported in ‰ relative to Vienna Standard MeanOceanWater (VSMOW). External reproducibility of replicate standard analysis was ±0.2‰ (1σ). The average oxygen isotope composition of the standard material NBS 120c was measured as 21.7‰.

4. Results

4.1. Foraminifers

Previously, Song et al. (2009) reported the occurrences of 16 foraminifer species belonging to 13 genera from the uppermost metres of the Talung Formation below the PTB at Bianyang. Our new detailed work in the Bianyang section provides an updated foraminiferal record. Diversity declines to eight foraminifera species (and 8 genera) recorded from a chert bed with carbonate lenses at the top of the Talung Formation (bed 3, Fig. 2), dated to belong to the *Clarkina yini* Zone (Yan et al., 2013). Diversity increases again in the overlying Luolou Formation, with abundant foraminifera found in two bioclastic limestone beds (beds 4 and 5, Fig. 2) of the *H. changxingensis* Zone (Yan et al., 2013). In total, 32 foraminifer species belonging to 24 genera are found in bed 4, whilst bed 5 contains 26 species belonging to 17 genera. None of those foraminifers are found at higher levels indicating a major extinction loss immediately below the PTB but above the main extinction level seen in most other South China section, which occurs at the top of the *C. yini* Zone.

4.2. Conodonts

Following the study of Yan et al. (2013), more samples have been processed for conodonts in order to get enough specimens for oxygen isotope analysis. This resulted in the discovery of the *Clarkina zhangi* and *Merillina ultima* in the *H. changxingensis* Zone. The typical Permian conodont *C. zhangi* normally appears below the mass extinction level, but at Bianyang it is found in the upper *H. cha*